Boulder Hazard Assessment of Potential Phoenix Landing Sites J. J. Marlow[1] C.R. Klein[2] M.M. Martinez[3] B.S. McGrane[4] and M.P. Golombek[5] [1]Washington University in St. Louis, jjmarlow@artsci.wustl.edu, [2]California Institute of Technology, cklein@its.caltech.edu [3]University of Washington, marleen@u.washington.edu [4]Occidental College, bmcgrane@oxy.edu [5]Jet Propulsion Laboratory, Caltech, mgolombek@jpl.nasa.gov

Introduction: The Phoenix Mars Lander will investigate the northern plains of Mars in June, 2008, searching for information concerning the origin and nature of ground ice, the possibility of liquid water, potential energy sources for life, past and present climatic processes, and the nature of the subsurface environment. In order to meet these objectives, a suitable landing site must be selected that allows for the study of ground ice and its interface with the Martian soil. Based on physical constraints on the landing site (such as dry layer thickness and altitude), three regions of interest were designated and labeled A, B, and C [1]. In order to better assess the relative risk of landing within each region, other hazards must be considered. This study evaluates the risk posed to the lander by one such threat: boulders visible from orbit.

Methods: Boulders were identified as anomalously low-albedo pixels in narrow angle Mars Orbiter Camera (MOC) images [2], an interpretation supported by the highest resolution (0.5 m/pixel) images. Confidence of boulder identification was highest in rock fields surrounding craters; these fields were used to calibrate our boulder identification techniques locally. Four independent observers identified 1176 boulder fields in 178 MOC images: 54 images in region A, 82 images in region B, and 42 images in region C. To provide a more quantifiable measure of risk, grayscale levels of each boulder field were manipulated such that only low albedo pixels interpreted to be boulders were visible. Field area and the percentage of pixels occupied by boulders, or the cumulative fractional area (CFA) were recorded.

Data and Results: The CFA data for boulder fields in each region shows significant variation among the regions (Fig. 1). Region A boulder fields have comparatively low CFAs, region B has the greatest variability, and region C has CFAs narrowly restricted to mid-range values.

A more succinct presentation of the data is provided in Table 1.

	Percent of All Area Covered by Fields	Percent of Boulder Field Area Occupied by Boulders	Percent of All Area Occupied by Boulders	Square Kilometers per Boulder Field
A	2.069	1.022	0.021	32.140
B	7.750	1.570	0.122	4.720
C	4.179	0.915	0.038	5.376
All	5.328	1.397	0.074	6.500

Table 1: Boulder field statistics by region

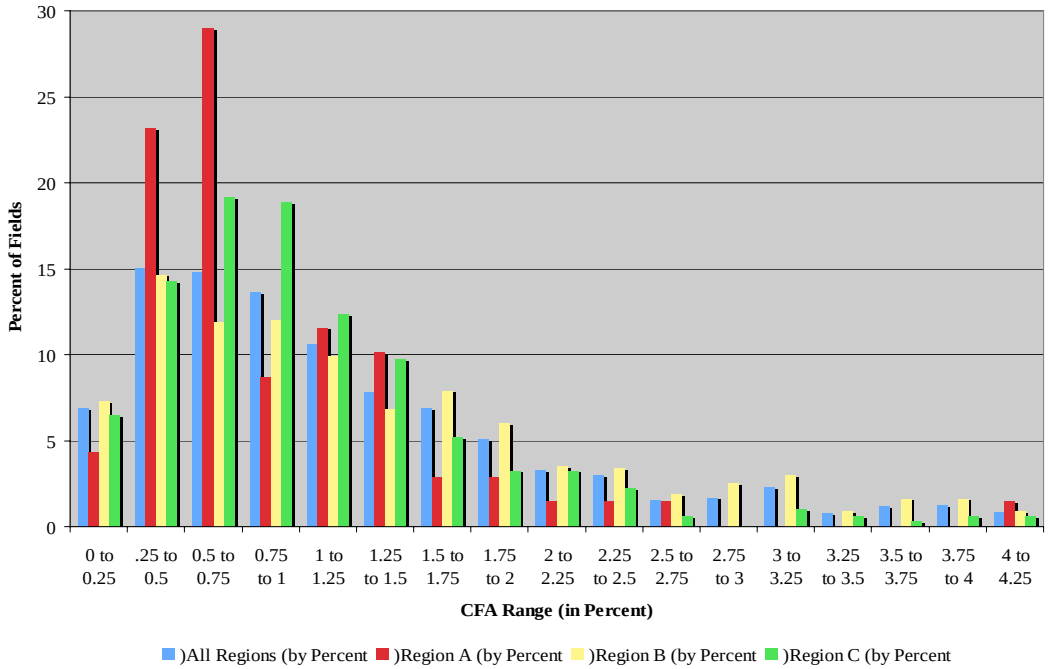

Figure 1: CFA histogram by region

Boulder fields cover a significantly smaller portion of the imaged area in region A, and cover the largest percentage of imaged area in region B. Within the fields themselves, region B has the largest ground coverage of boulders, while regions A and C have smaller and comparable values. The percentage of all visible area occupied by boulder pixels is several times larger in region B than in the other regions, but it is important to note that all values are extremely small (<0.13% of all imaged area is occupied by boulders).

Cumulative Number. In order to extract meaningful data such as the probability of boulder impact upon landing, the cumulative number (CN) of boulders of a particular size and greater per unit area was obtained. This was done via size frequency counts, a procedure that tabulates the number of boulders of each observed size [3,4]. Such counts were obtained by counting the number of low albedo pixels for each boulder in the field and calculating the boulder diameter from the area of a boulder (number of pixels) of representative boulder fields in all three regions. Using the 39 representative regions counted, a plot of CFA vs. the total CN was generated. The graph was found to have a relatively linear correlation, which allowed the derivation of the cumulative number of boulders of a given size or larger from the measured CFA for statistical analysis.

Boulder Probabilities. The Phoenix lander has legs that provide 0.33-0.45 m of clearance over a 1.75 square meter area and solar arrays that sweep out a 6 square meter area with 0.5 m clearance. Because MOC image resolution is typically around 3 m/pixel, all boulders (assumed to be hemispheres) observed were considered hazardous to landing and opening of the solar panels.

Upon derivation of CN values from previously determined CFAs, the probability of encountering a boulder was calculated using the method of Golombek et al. [4]. Probabilities of "lander" and "lander plus array" boulder impacts were calculated for several CN values.

Color Coding. In order to best portray relative risk posed to the lander on a field-by-field basis, a color code was established. According to this classification system, green regions signify fields with the lowest CFA, CN, and impact probability values. Yellow, orange, and red colored fields represent areas of increasing risk. Boundaries between regions were drawn primarily at observed breaks in the CFA, CN plotted distribution.

Results of probability analyses for the color coded regions shown in Table 2 indicate that the probability of landing on a boulder in a boulder field is very small (<0.07% for green fields, <0.13% for yellow fields, <0.29% for orange fields and >0.29% for red fields). The probability of landing on or encountering a rock that would impede solar array opening is larger, but still small (<0.32% for green fields, <0.56% for yellow fields, <1.29% for orange fields and >1.29% for red fields). Because the total area occupied by boulder fields in existing high-resolution MOC images is only 2-8%, the probability of impacting a boulder in the landing region would be substantially smaller.

This analysis suggests that large boulders visible from orbit in MOC images do not represent a significant risk to the Phoenix Mars lander.

References: [1] Arvidson, R., et al., 37th LPSC abs., 2006. [2] Malin, M., and K. Edgett, JGR, *106*, 23,429-23,570, 2001. [3] Golombek, M., and Rapp, D., JGR *102*, 4117-4129, 1997. [4] Golombek, M. P., et al., JGR *108*(E12), 8086, doi:10.1029/2002 JE002035, 2003.

Significance	Color	CN value	Associated CFA	Lander prob %	Lander + array %
green avg	green	0.000246	0.00399	0.04	0.19
boundary	green	0.00041	0.00679	0.07	0.32
yellow avg	yellow	0.000566	0.00919	0.1	0.44
boundary	yellow	0.00073	0.0119	0.13	0.56
orange avg	orange	0.001077	0.0175	0.19	0.83
boundary	orange	0.00167	0.0271	0.29	1.29
red avg	red	0.00295	0.0481	0.52	2.26

Table 2: Risk values by color region